SUPPLEMENTAL MATERIAL

Supplemental Methods

Animals

We used 3-5 month-old mice (male and female mice were used for pMCAO; male mice were used for infarct volumetry experiments), which were housed in groups (two to five per cage) on a 12-h light/dark cycle with food and water available ad libitum. *Cx43-ECFP* (1) and *Ip3r2-/-* (also known as *Itpr2-/-*) (2) mice have been described previously. *Cx43-ECFP* mice were provided by M. Theis (University of Bonn, Germany), and *Ip3r2-/-* were provided J. Chen (University of California, San Diego). All mouse lines were backcrossed to the C57BL/6N background for >10 generations.

Stroke models

For MCAO, the mouse was placed on its back and an incision was made above the thyroid gland. The left common carotid artery was separated from the surrounding tissue and the vagus nerve, and ligated with a suture 3-4 mm proximal to the bifurcation. Following a second ligation around the external carotid artery distal to the bifurcation and application of a vascular clamp (Fine Science Tools) around the internal carotid artery, a small incision was made in the common carotid artery and the filament for pMCAO induction was inserted (9-10 mm coating length, 0.19 ± 0.01 mm tip diameter; Doccol). After removal of the clip, the filament was pushed forward until it occluded the middle

cerebral artery, and fixed in place with a suture. For transient MCAO, the filament was removed after 60 min.

For photothrombotic focal ischemia (3), we intravenously injected the photosensitive dye Rose Bengal (30 mg/kg; Sigma). Five minutes after the injection, we illuminated the left sensorimotor cortex with an LED (515 nm) through an optical fiber (Doric Lenses) for 15 min.

Cranial window surgery and multiphoton microscopy

Cranial windows were prepared as described (4). Briefly, animals were anesthetized with isoflurane (induction, 3 %; maintenance, 1-1.5% v/v) and kept on a heating plate (37 °C). After fixation in a stereotaxic frame, the scalp was removed and a craniotomy was created above the left somatosensory cortex (centered at 2.5 mm lateral and 1.5 mm posterior to bregma) using a dental drill. Agarose (1.5 %) was placed on top of the cortex for stabilization and the window was closed with a cover glass.

OGB-1 AM (Invitrogen) or Cal-590 (AAT Bioquest) were solubilized in 20 % Pluronic and 80 % DMSO (Biotium) and diluted to 1 mM with PBS. The dyes were bulk-loaded (5) into the cortex of anesthetized mice at a depth of 80-130 μm using glass micropipettes (4-6 μm tip diameter; WPI) connected to a pneumatic injector (0.2-0.5 bar, 30-60 s; PDES, NPI Electronic). Alexa Fluor 633 (2 mg/kg in saline; Invitrogen) and dextran-coupled Texas Red (70 kDa, 5 % in saline, 100 μl; Invitrogen) were injected intravenously. Mice were kept on a homeothermic heating pad, and the level of anesthesia was assessed by tail pinch tests. Mice were imaged through cranial windows using an upright two-photon microscope (LaVision Trim ScopeII) with a 20x objective

(1.0 numerical aperture; Zeiss) and three non-descanned detectors (460-500 nm for ECFP, either 500-550 nm for iGluSnFR or 520-550 nm for OGB-1, and either 635-675 nm for Alexa 633 or >585 nm for Texas Red dextran and Cal-590). Fluorophores were excited at 880 nm (ECFP, OGB-1, Texas Red dextran) or 950 nm (iGluSnFR and Cal-590) using a Ti:Sapphire laser (Chameleon Ultra II, pumped by an 18 W laser; Coherent). Laser power below the objective was kept between 20 and 40 mW to minimize laser-induced artefacts and phototoxicity. Z stacks of the imaging region were taken, and XY time-lapse series (3 Hz) of spontaneous calcium activity and blood vessels were subsequently recorded at a depth of 100-150 μm beneath the surface. For high temporal and spatial resolution time-lapse series, images were acquired at 10 Hz. MPEP (100 μM; Tocris) and LY341495 (50 μM; Tocris) were solubilized in PBS and topically applied to the cortex.

Line scans along the longitudinal axis of capillaries in the imaging region before and after pMCAO induction were recorded at 500 Hz for 30 s to determine erythrocyte velocity and flux. Each band in the space-time matrix corresponds to a red blood cell propagating through the fluorescently labeled plasma, with changes in slope of the bands indicating velocity changes and changes in the number of bands corresponding to alterations in erythrocyte flux. Because shifts in the Z direction during PIDs prevented the measurement of passage of single erythrocytes through cortical capillaries by line scanning, we instead identified penetrating cortical arterioles by their specific labeling with Alexa Fluor 633 (6) and measured their diameter changes during PIDs after labeling with Texas Red dextran.

Virus injections

Virus was injected into the cortex of anesthetized mice through a small burrhole using a glass micropipette (6 μm tip diameter; WPI) connected to a pneumatic injector (PDES, NPI Electronic). 1μl of AAV2/5.GFAP.iGluSnFR.WPRE.SV40 (#AV-5-PV2914, University of Pennsylvania Vector Core, Philadelphia) was injected for 1 min, and the glass pipette was left in place for 2 min. The hole was covered with bone wax and surgical wounds were closed with external sutures, and animals were allowed to recover in a warmed recovery chamber (V1200, Peco). Lidocaine and buprenorphine were administered as analgesics.

Laser speckle contrast imaging

After cranial window preparation, anesthetized mice were fixed in a stereotaxic frame and placed under the laser speckle contrast imaging system (PeriCam PSI, Perimed). Relative CBF changes were measured using PimSoft software (Perimed) at a resolution of 60 μm/pixel. Baseline CBF was recorded for 5 min, followed by pMCAO induction.

Electrophysiology

The cranial window was temporarily covered with a glass coverslip sealed with a removable silicone elastomer (Kwik-Cast, WPI) for pMCAO induction. Subsequently, the anesthetized mouse was fixed in a stereotaxic frame, and elastomer and coverslip were removed. A borosilicate glass microelectrode (tip diameter, 2-5 μm; WPI) connected to a head stage (EXT-02, NPI Electronic) was inserted 100-200 μm below the pial surface from an oblique angle; a reference electrode was placed subcutaneously at

the neck. The window was subsequently closed again with a coverslip. The DC potential was amplified (EXT-02F/2, NPI Electronic), and filtered at 3-30 Hz. A laser Doppler probe (VMF-LDF2, Moor) was placed at a distance of 3-5 mm to the electrode. Both signals were digitized (micro1401, CED), and analyzed offline using Spike2 (CED).

Histology

Anesthetized mice were fixed with 4 % paraformaldehyde 72 h after transient MCAO. After cryopreservation, 20-µm coronal sections were cut using a cryostat (Leica). Brain sections spaced 280 µm apart were stained with cresyl violet (Fisher Scientific) for infarct volumetry. Separate sections from the infarct area were stained with Fluoro-Jade C staining (Merck) according to the manufacturer's instructions.

Data analysis

All data analysis was conducted in a blinded fashion with respect to genotype. For calcium imaging data analysis, time-lapse series were imported into ImageJ 1.50 (W. Rasband, NIH, Bethesda), and stabilized using the Image Stabilizer plugin for ImageJ (K. Li, Carnegie Mellon University, Pittsburgh). Cells positive for OGB-1 were considered astrocytes when they expressed ECFP. Neuronal somata were manually identified by their morphology and the absence of ECFP, while astrocytic somata were identified semi-automatically using a custom-written ImageJ algorithm. Fluorescence over time was determined for each region of interest (ROI), converted to $\Delta F/F$, and imported into Matlab (Mathworks). After removal of outliers using a median filter and smoothing using a Gaussian filter, peak amplitude, time to peak, peak to baseline, and FDHM were

determined for each signal using a custom-written algorithm in Matlab. Calcium elevations were defined as signals when fluorescence increased ≥ 2 s.d. relative to baseline fluorescence (i.e. 100 data points preceding the signal increase). In addition, $\Delta F/F$ in each ROI was plotted together with the respective video file for visual inspection and verification. Signal propagation velocity was calculated by dividing the distance between somata spaced ≥ 100 µm apart by the time lag between the onset of calcium signals.

For analysis of glutamate kinetics, ROIs corresponding to individual iGluSnFR-expressing astrocytes were semi-automatically identified using the GECIquant plugin for ImageJ (7). Intensity changes over time for each ROI were also determined using GECIquant, imported into Matlab, and analyzed as described above. Calcium changes in iGluSnFR-positive astrocytes were determined by measuring Cal-590 signal changes within the same ROI using the same algorithm.

Erythrocyte velocity was calculated from line scan data as described (8), using an automated Matlab algorithm that was modified from a routine provided to us by N. Nishimura (Cornell University, Ithaca) (9). Arteriolar diameter over time was determined after image stabilization, resizing and 3D smoothing in ImageJ, using a custom-written Matlab algorithm. Relative changes in CBF were estimated using Hagen-Poiseuille's law (assuming constant pressure drop, viscosity and vessel length during the imaging period). Infarct volume was calculated by numerically integrating lesion areas on Nissl-stained brain sections after edema correction (10). The density of dead neurons on sections stained with Fluoro-Jade C was calculated using ImageJ. After applying a Gaussian blur (sigma = 1 µm) and normalization (saturated pixels, 0.4 %), images were binarized using

the MaxEntropy algorithm of the Auto Threshold function, and neurons positive for Fluoro-Jade C were automatically counted in ROIs.

Supplemental References

1. Degen J et al. Dual reporter approaches for identification of Cre efficacy and astrocyte heterogeneity. *FASEB J.* 2012;26(11):4576–4583.

2. Li X, Zima AV, Sheikh F, Blatter LA, Chen J. Endothelin-1-induced arrhythmogenic Ca2+ signaling is abolished in atrial myocytes of inositol-1,4,5-trisphosphate(IP3)-receptor type 2-deficient mice. *Circ Res.* 2005;96(12):1274–1281.

3. Watson BD, Dietrich WD, Busto R, Wachtel MS, Ginsberg MD. Induction of reproducible brain infarction by photochemically initiated thrombosis. *Ann Neurol.* 1985;17(5):497–504.

4. Delekate A, Füchtemeier M, Schumacher T, Ulbrich C, Foddis M, Petzold GC. Metabotropic P2Y1 receptor signalling mediates astrocytic hyperactivity in vivo in an Alzheimer's disease mouse model. *Nature Commun.* 2014;5:5422.

5. Stosiek C, Garaschuk O, Holthoff K, Konnerth A. In vivo two-photon calcium imaging of neuronal networks. *Proc Natl Acad Sci USA.* 2003;100(12):7319–7324.

6. Shen Z, Lu Z, Chhatbar PY, O'Herron P, Kara P. An artery-specific fluorescent dye for studying neurovascular coupling. *Nat Methods.* 2012; 9(3):273–276.

7. Srinivasan R et al. Ca2+ signaling in astrocytes from Ip3r2−/− mice in brain slices and during startle responses in vivo. *Nat Neurosci.* 2015;18(5):708–717.

8. Petzold GC, Albeanu DF, Sato TF, Murthy VN. Coupling of neural activity to blood flow in olfactory glomeruli is mediated by astrocytic pathways. *Neuron.* 2008;58(6):897–910.

9. Schaffer CB et al. Two-photon imaging of cortical surface microvessels reveals a robust redistribution in blood flow after vascular occlusion. *PLoS Biol.* 2006;4(2):e22.

10. Ginsberg MD et al. Stilbazulenyl nitrone, a novel antioxidant, is highly neuroprotective in focal ischemia. *Ann Neurol.* 2003;54(3):330–342.

Supplemental Figures and Movie
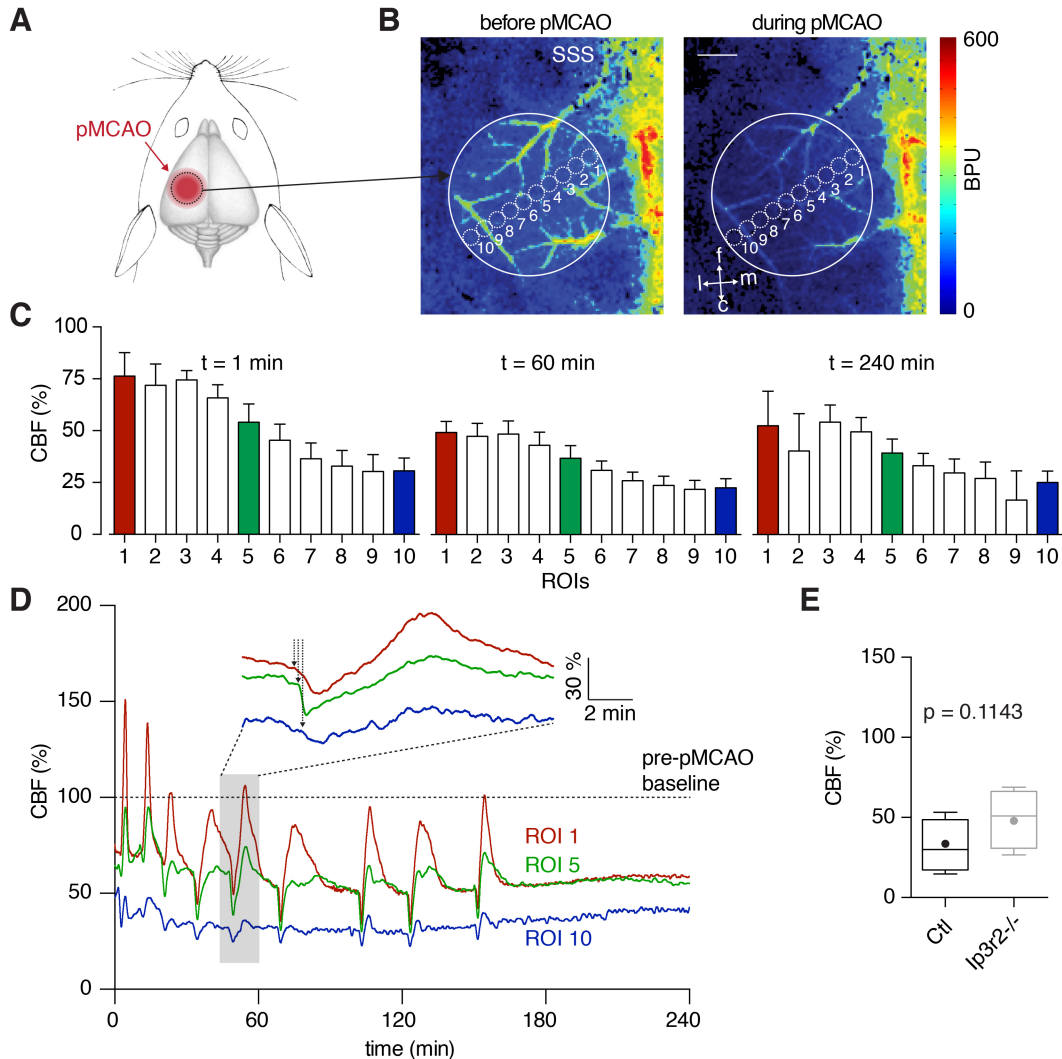
Supplemental Figure 1. Identification of peri-infarct cortex and peri-infarct depolarizations (PIDs).
(A) We defined the peri-infarct zone as a CBF range of ~20-40 % relative to baseline. To identify this area in mice, we created closed cranial windows above the sensorimotor cortex in wildtype mice and subjected them to pMCAO. **(B)** Relative CBF changes were determined using laser speckle contrast imaging by placing ROIs (1-10) in the cortex that spanned the mediolateral axis of the window (f, frontal; c, caudal; l, lateral; m, medial; SSS, superior saggital sinus). By mapping CBF changes in these ROIs with high temporal and spatial resolution, a drop in perfusion could be seen after pMCAO induction

(BPU, arbitrary blood perfusion units). Scale bar, 1 mm. **(C)** Relative perfusion changes normalized to baseline (before pMCAO) in ROIs 1-10 immediately after pMCAO (1 min) as well as after 60 min and 240 min (n = 4 mice; data are shown as mean ± s.e.m.). Depending on the mediolateral position of each ROI, regional CBF dropped to values between 76.3 ± 22.7 % in the most medial ROI and 30.6 ± 12.3 % in the most lateral ROI relative to baseline (=100 % before pMCAO induction) immediately after pMCAO induction, between 49.2 ± 10.7 % and 22.6 ± 8.8 % after 60 min, and between 52.4 ± 33.4 % and 25.1 ± 11.1 % after 4 h, respectively. Based on these measurements, we defined the peri-infarct zone in our model as the area 2.5-3 mm lateral and 1.5 mm posterior to the bregma, corresponding to ROIs 5-10, in which CBF consistently remained between ~25 % and ~35 % after pMCAO during our experiments. **(D)** We detected the typical cerebrovascular signature of PIDs during pMCAO in peri-infarct cortex, consisting of a hypoperfusion and a subsequent variable hyperemia. The severity of hypoperfusion and hyperemia during PIDs depended on the level of ischemia in the tissue: Hypoperfusion was relatively short-lived and followed by pronounced hyperemia in mildly hypoxic tissue (ROI 1, corresponding to the medial part of the window), while hypoperfusion became more severe and hyperemia became attenuated as PIDs propagated into more hypoxic tissue (ROI 5, green; ROI 10, blue). Different times of onset, visualized by arrows in the inset, demonstrate the propagating nature of the event. **(E)** The level of ischemia in peri-infarct cortex was similar between *Ip3r2-/-* and wildtype mice (n = 5 mice in each group; Mann-Whitney test).
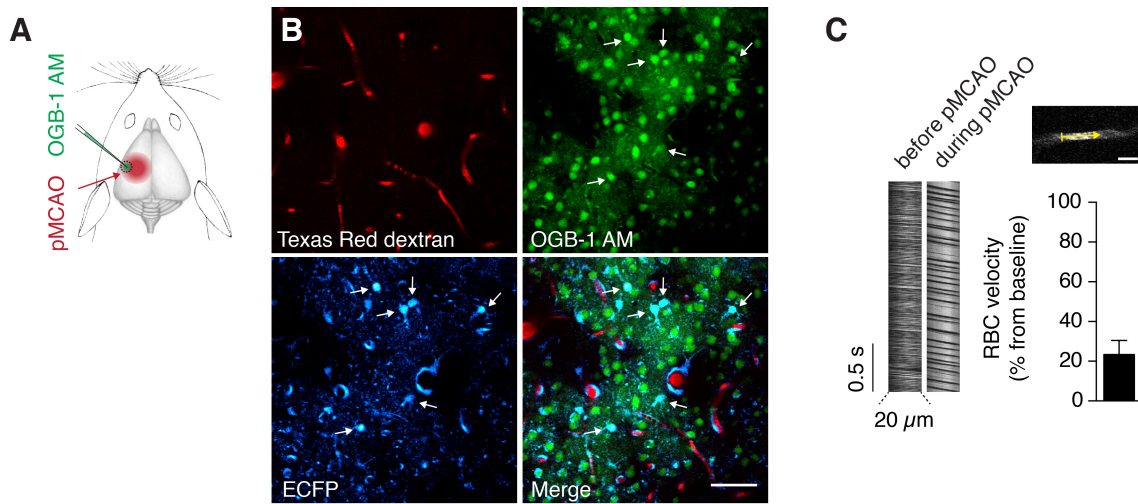
Supplemental Figure 2. Multiphoton imaging of astroglial and neuronal calcium and the vasculature in peri-infarct cortex.

(A-B) The calcium indicator OGB-1 AM was injected into peri-infact cortex, and mice expressing ECFP under the Cx43 promoter were imaged using multiphoton microscopy before and after pMCAO. Astrocytes were identified by their co-labeling with ECFP and OGB-1 (arrows). The vasculature was labeled with Texas Red dextran. Scale bar, 50 µm. **(C)** Line scans along the longitudinal axis of capillaries in the imaging region confirmed the drop in CBF after pMCAO. Each band corresponds to a red blood cell (RBC) propagating through the labeled plasma. The velocity decrease is indicated by the change in slope of the bands. The number of RBCs (i.e. flux), indicated by the number of bands, also decreases after pMCAO. The yellow arrow indicates direction and path length of the line scan (scale bar, 10 µm). On average, RBC velocity decreased to 23.3 ± 7.1 % from baseline (n = 5 mice; data are shown as mean ± s.e.m.).
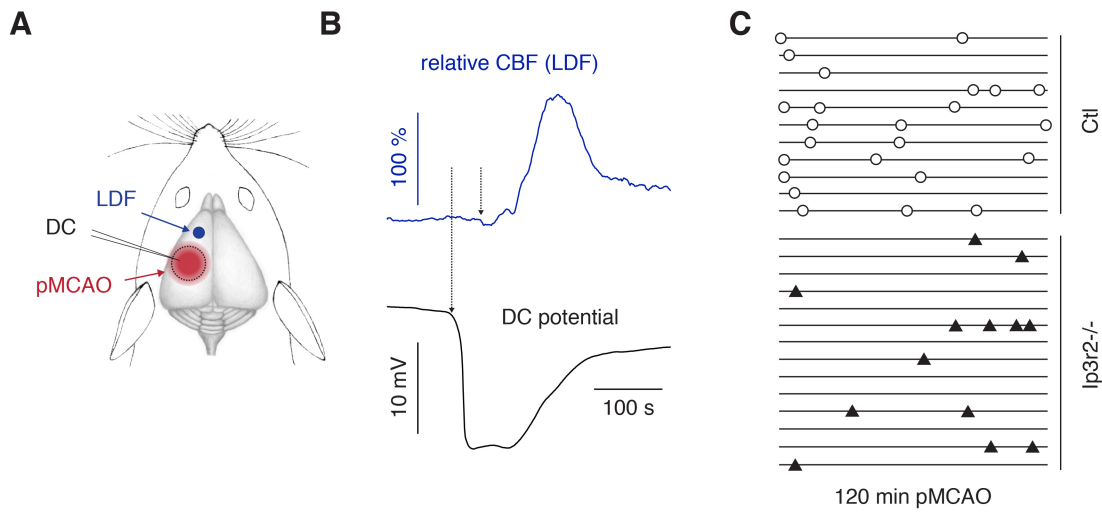
Supplemental Figure 3. Electrophysiological recordings of PIDs in *Ip3r2-/-* and wildtype mice.
(A-B) A microelectrode was inserted into peri-infarct cortex to measure direct current (DC) potential changes during PID. To confirm the propagating nature of each event, a laser Doppler flow (LDF) probe was positioned over healthy cortex. DC potential changes during PID consisted of a negative deflection that was followed by a hyperemic CBF response (dashed arrows indicate the time lag between the two signals). **(C)** Comparison of PIDs in control mice (white circles) and in *Ip3r2-/-* mice (black triangles). Each horizontal line represents one animal.
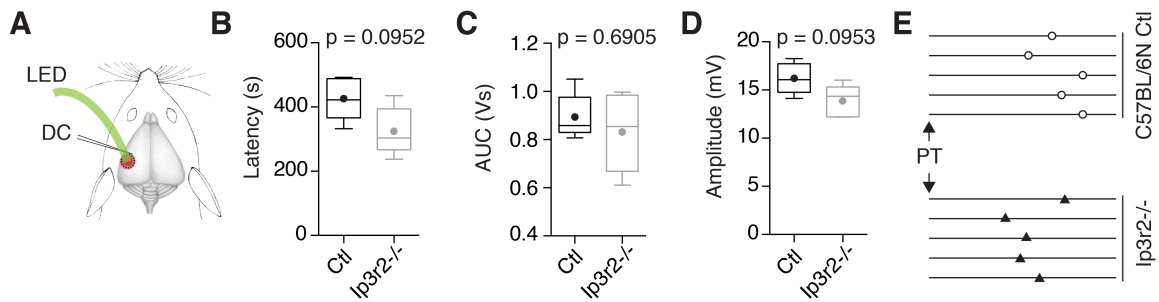
Supplemental Figure 4. Similar initial ischemic depolarization in *Ip3r2-/-* and wildtype mice.

Photothrombotic stroke (rather than MCAO) was used to study the initial ischemic depolarization to precisely time the onset of ischemia. **(A)** Following intravenous Rose Bengal injection, we induced focal photothrombotic stroke by LED illumination of a focal area in the cortex after a glass electrode had been placed in peri-infarct cortex to measure the direct current (DC) potential. **(B-D)** There were no differences in latency, area under the curve (AUC) and amplitude of the initial depolarization in *Ip3r2-/-* vs. C57BL/6N control mice (n = 5 mice in each group; Mann-Whitney test). **(E)** Visual comparison of initial depolarizations after photothrombosis (PT) in control mice (white circles) and in *Ip3r2-/-* mice (black triangles). Each horizontal line (10 min) represents one animal.
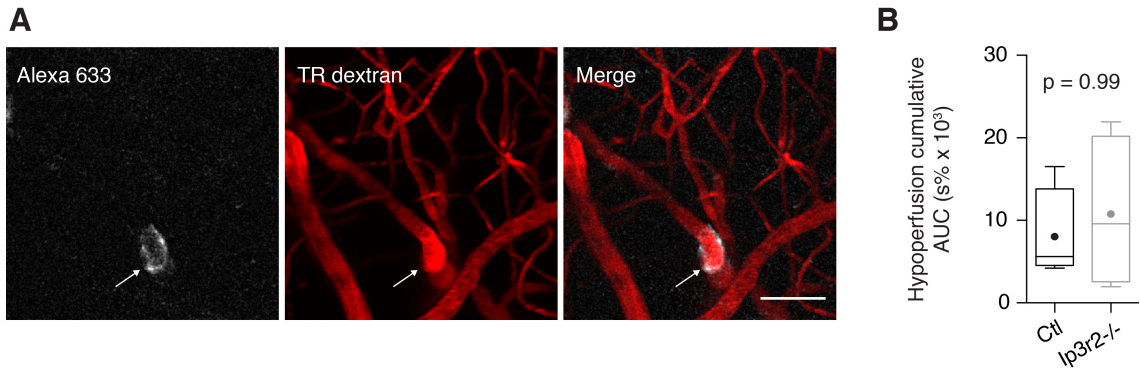
Supplemental Figure 5. Blood flow changes during PIDs.
(A) Penetrating arterioles were identified by their labeling with Alexa 633 in multiphoton imaging experiments (arrow; the plasma was labeled with Texas Red (TR) dextran). Scale bar, 50 μm. **(B)** There was no significant difference in the cumulative area under the curve (AUC) of the PID-related hypoperfusion measured by laser speckle contrast imaging within 4 h after MCAO induction (n = 4 mice in each group; Mann-Whitney test).
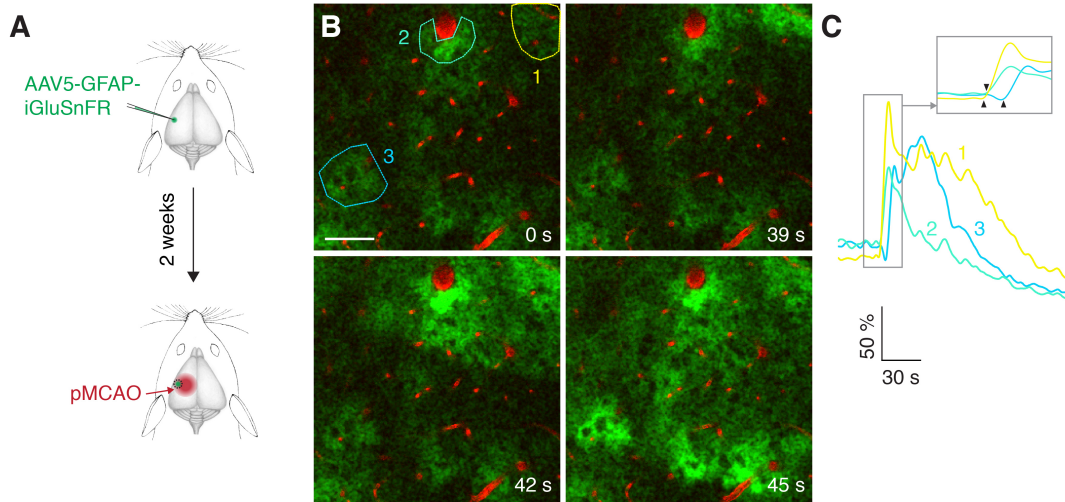
Supplemental Figure 6. Astrocyte-specific expression of iGluSnFR reveals a glutamate increase near astrocytes during PIDs.
(A) Adeno-associated virus (AAV) vector encoding the fluorescent glutamate sensor iGluSnFR driven by the astrocyte-specific GFAP promoter was injected into the cortex. Two weeks later, mice were subjected to pMCAO and imaged using multiphoton microscopy. **(B)** PIDs led to a wave of propagating glutamate increase near astrocytes (images are from the same animal as in Figure 3A). Scale bar, 50 µm. Representative glutamate transients for astrocytes marked **1**-3 are given in **C**, with the inset demonstrating propagation (arrowheads). The glutamate increase consisted of a sharp rise phase, followed by a sustained secondary increase.

Supplemental Movie 1. Identification of astrocytes by their expression of enhanced cyan fluorescent protein (ECFP) in *Cx43-ECFP* mice.
Z stack of 3 merged channels: ECFP-positive astrocytes (blue), OGB-1-labeled astrocytes and neurons (green) and Texas Red-labeled vasculature (red).

Supplemental Movie 2. Time-lapse series of calcium changes in the astroglial-neuronal network labeled with OGB-1 AM during peri-infarct depolarizations. A PID entered the field of view from the right and was associated with calcium elevations in individual cells, as indicated by an increase in the fluorescence of OGB-1 (green). Astrocytes can be identified by their expression of ECFP (blue). The vasculature is visualized with Texas Red dextran (red).